

Efficient Conditional Pre-training for Transfer Learning

Shuvam Chakraborty
Department of Computer Science
Stanford University
shuvamc@stanford.edu

Kumar Ayush
Department of Computer Science
Stanford University
kayush@stanford.edu

Evan Sheehan
Department of Computer Science
Stanford University
esheehan@stanford.edu

Burak Uzkent
Department of Computer Science
Stanford University
buzkent@cs.stanford.edu

Kumar Tanmay
Department of Computer Science
IIT Kharagpur
kr.tanmay147@iitkgp.ac.in

Stefano Ermon
Department of Computer Science
Stanford University
ermon@cs.stanford.edu

Abstract

Almost all the state-of-the-art neural networks for computer vision tasks are trained by (1) pre-training on a large-scale dataset and (2) finetuning on the target dataset. This strategy helps reduce the dependency on the target dataset and improves convergence rate and generalization on the target task. Although pre-training on large-scale datasets is very useful, its foremost disadvantage is high training cost. To address this, we propose efficient target dataset conditioned filtering methods to remove less relevant samples from the pre-training dataset. Unlike prior work, we focus on efficiency component of filtering as well as transfer learning performance. Additionally, we discover that lowering image resolutions in the pre-training step offers a great trade-off between cost and performance. We validate our techniques by pre-training on ImageNet in both the unsupervised and supervised settings and finetuning on a diverse collection of target datasets and tasks. Our proposed methods drastically reduce pre-training cost and provide strong performance boosts.

1. Introduction

Despite recent successes, many modern computer vision methods rely heavily on large scale labeled datasets, which are often costly and time-consuming to collect [27, 15, 4]. Alternatives to reducing dependency on large scale labelled data include pre-training a network on the publicly available

ImageNet dataset with labels [8]. It has been shown that ImageNet features can transfer well to many different target tasks [21, 45, 34, 19, 23]. Another alternative, unsupervised learning, has received tremendous attention recently with the availability of extremely large scale data with no labels, as such data is costly to obtain [27]. It has been shown that recent unsupervised learning methods, e.g. contrastive learning, can perform on par with their supervised learning counterparts [15, 16, 12, 2, 3, 4]. Additionally, it has been shown that unsupervised learning methods perform better than pre-training on ImageNet on various downstream tasks [15, 16, 4, 33, 38]

The explosion of data quantity and improvement of unsupervised learning portends that the standard approach in future tasks will be to (1) learn weights on a very large scale dataset with unsupervised learning and (2) finetune the weights on a small-scale target dataset. A major problem with this approach is the large amount of computational resources required to train a network on a very large scale dataset [27]. For example, a recent contrastive learning method, MoCo-v2 [16, 15], uses 8 Nvidia-V100 GPUs to train on ImageNet-1k for 53 hours, which can cost thousands of dollars. Extrapolating, this forebodes pre-training costs on the order of millions of dollars when considering much larger-scale datasets. Those without access to such resources will require selecting relevant subsets of those datasets. However, other studies that perform conditional filtering, such as [46, 7, 28, 11], do not take efficiency into account at all.

Cognizant of these pressing issues, we first investigate

the use of low resolution images for pre-training, which improves efficiency by 30-50% with minimal performance loss. We also propose novel methods to efficiently *filter* a user defined number of pre-training images conditioned on a target dataset. Our approach consistently outperforms baselines by up to 10% of accuracy/average precision. Due to our focus on filtering based on image features, not labels, our methods are flexible, translating to both supervised and unsupervised settings, and adaptable, translating to a wide range of target tasks. Due to our focus on features, our methods perform especially well in the more relevant unsupervised setting, where pre-training on a small fraction of data achieves close to full pre-training target task performance.

2. Related Work

Active Learning The goal in active learning is to fit a function by selectively querying labels for samples where the function is currently uncertain. In a basic setup, the samples with the highest entropies are chosen for annotation [42, 10, 1, 32]. The model is iteratively updated with these samples and accordingly selects new samples. Active learning typically assumes similar data distributions for candidate samples, whereas our data distributions can potentially have large shifts. Furthermore, active learning, due to its iterative nature, can be quite costly, hard to tune, and can require prior distributions [29].

Unconditional Transfer Learning The success of deep learning on datasets with increased sample complexity has brought transfer learning to the attention of the research community. Pre-training networks on ImageNet-1k has been shown to be a very effective way of initializing weights for a target task with small sample size [21, 45, 34, 19, 23, 39, 37]. However, all these studies use unconditional pre-training as they employ the weights pre-trained on the full ImageNet dataset for any target task, and, as mentioned, full pre-training on large scale data could be prohibitively costly.

Conditional Transfer Learning [46, 7, 28], on the other hand, filter the pre-training dataset conditioned on target tasks. In particular, [7, 11] use greedy class-specific clustering based on feature representations of target dataset images. To learn image representations, they use an encoder trained on the massive JFT-300M dataset [20]. It should be highlighted that pre-training on JFT-300M dataset to learn encoder for filtering source images dramatically increases complexity. [46] trains a number of expert models on many subsets of the pre-training dataset. Source images are assigned high importance weights if they are used for the training of an expert with a good target task performance. However, this method is computationally expensive as it requires training many experts on different subsets of the pre-training dataset and fine-tuning them on the target dataset to

assign importance weights to source images.

Our methods differ from the past works as we take into account both pre-training dataset filtering efficiency and target task performance.

3. Problem Definition and Setup

We assume a target task dataset represented as $\mathcal{D}_t = (\mathcal{X}_t, \mathcal{Y}_t)$ where $\mathcal{X}_t = \{x_t^1, x_t^2, \dots, x_t^M\}$ represents a set of M images with their ground truth labels \mathcal{Y}_t . Our goal is to train a function f_t parameterized by θ_t on the dataset \mathcal{D}_t to learn $f_t : x_t^i \mapsto y_t^i$. One strategy is using randomly initialized weights for θ_t , but a better recipe exists for a small size dataset \mathcal{D}_t . In this case, we first pre-train θ_t on a large-scale source dataset \mathcal{D}_s and fine-tune θ_t on \mathcal{D}_t . This strategy not only reduces the amount of labeled samples needed in \mathcal{D}_t but also boosts the accuracy in comparison to the randomly initialized weights [27, 38]. For the pre-training dataset, we can have either labelled or unlabelled setups: (1) $\mathcal{D}_s = (\mathcal{X}_s, \mathcal{Y}_s)$ and (2) $\mathcal{D}_s = (\mathcal{X}_s)$ where $\mathcal{X}_s = \{x_s^1, x_s^2, \dots, x_s^N\}$. The most common example of the labelled setup is the ImageNet dataset [8]. However, it is tough to label vast amounts of publicly available images, and with the increasing popularity of unsupervised learning methods [4, 5, 3, 15, 16], it is easy to see that unsupervised pre-training on very large \mathcal{D}_s with no ground-truth labels will be the standard and preferred practice in the future.

A major problem with learning θ_t on a very large-scale dataset \mathcal{D}_s is the computational cost, and using the whole dataset may be impossible for most. One way to reduce costs is to filter out images deemed less relevant for \mathcal{D}_t to create a dataset $\mathcal{D}'_s \in \mathcal{D}_s$ where $\mathcal{X}_s = \{x_s^1, x_s^2, \dots, x_s^{N'}\}$ represents a filtered version of \mathcal{D}_s with $N' \ll N$. Our approach conditions the filtering step on the target dataset \mathcal{D}_s . In this study, we propose flexible and adaptable methods to perform *efficient conditional pre-training*, which reduces the computational costs of pre-training and maintains high performance on the target task.

4. Methods

We investigate a variety of methods to perform efficient pretraining while attempting to minimize accuracy loss on the target dataset. We visualize our overall technique in Figure 1 and explain our techniques below.

4.1. Conditional Data Filtering

We propose two novel methods to perform conditional filtering efficiently. Our methods score every image in the source domain and select the best scoring images according to a pre-specified data budget N' . Our methods are fast, as they require at most one forward pass through \mathcal{D}_s to get the filtered dataset \mathcal{D}'_s and furthermore can work on both $\mathcal{D}_s = (\mathcal{X}_s, \mathcal{Y}_s)$ and $\mathcal{D}_s = (\mathcal{X}_s)$. The fact that we consider *data*

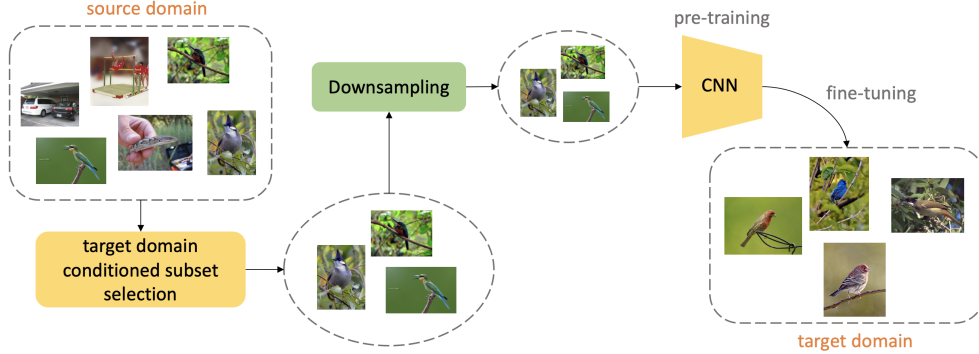


Figure 1: Schematic overview of our approach. We first perform a conditional filtering method on the source dataset then downsize image resolution on this filtered subset. Finally, we perform pre-training on the subset and finetuning on the target task.

features not labels perfectly lends our methods to the more relevant unsupervised setting. This is in contrast to previous work such as [7, 11, 28] which do not consider efficiency and are designed primarily for the supervised setting and thus will be more difficult for most to apply to large scale datasets.

Algorithm 1 Clustering Based Filtering

- 1: **procedure** CLUSTERFILTER($\mathcal{D}_s, \mathcal{D}_t, N', K, \text{AggOp}$)
 - 2: $f_h \leftarrow \text{TRAIN}(\mathcal{D}_t)$ ▷ Train Feature Extractor
 - 3: $\mathcal{Z}_t \leftarrow \{f_h(x_t^i)\}_{i=1}^M$ ▷ Target Representations
 - 4: $\{\hat{z}\}_{k=1}^K \leftarrow K\text{-Means}(\mathcal{Z}_t, K)$ ▷ Cluster Target
 - 5: $d_k^i(x_s^i, k) \leftarrow \|f_h(x_s^i) - \hat{z}_k\|_2$
 - 6: $c_s \leftarrow \{\text{AggOp}(\{d_k^i\}_{k=1}^K)\}_{i=1}^{N'}$ ▷ Score
 - 7: $\mathcal{D}'_s \leftarrow \text{BOTTOM}(\mathcal{D}_s, N', c_s)$ ▷ Filter Source
 - 8: **return** \mathcal{D}'_s ▷ Return the Filtered Subset
-

4.1.1 Conditional Filtering by Clustering

Selecting an appropriate subset \mathcal{D}'_s of pre-training data \mathcal{D}_s can be viewed as selecting a set of data that minimizes the Earth Mover Distance (or 1-Wasserstein distance) between \mathcal{D}'_s and the target dataset \mathcal{D}_t , as explored in [7, 11]. This is accomplished by taking feature representations \mathcal{Z}_s of the set of images \mathcal{X}_s and selecting pre-training image classes which are close (by some distance metric) to the representations of the target dataset classes.

Our method can be interpreted as an extension of this high level idea (i.e. minimizing distance between datasets), but we make several significant modifications to account for our goals of efficiency and application to unsupervised settings.

Training Only with Target Data. We do not train a network f_h on a large scale dataset, i.e. JFT-300M [7], as this defeats the entire goal of pre-training efficiency. Therefore,

we first train a model f_h with parameters θ_h using the target dataset $\mathcal{D}_t = (\mathcal{X}_t, \mathcal{Y}_t)$ and use the learned θ_h to filter source dataset \mathcal{D}_s .

Consider Source Images Individually. Selecting entire classes of pre-training data is inefficient and wasteful when limited to selecting a small subset of the data. For example, if limited to 6% of ImageNet, (a reasonable budget for massive datasets), we can only select 75 of the 1000 classes, which may prohibit the model from having the breadth of data needed to learn transferrable features. Instead, we treat each image x_s^i from \mathcal{D}_s separately to flexibly over-represent relevant classes while not being forced to wholesale select entire classes. Additionally, very large scale datasets may not have class labels \mathcal{Y}_s . For this reason, we want to develop methods that work with unsupervised learning, and treating source images independently accomplishes this.

Scoring and Filtering. Finally, we choose to perform K-Means clustering on the representations \mathcal{Z}_t learned by f_h to get K cluster centers $\{\hat{z}\}_{k=1}^K$. We then compute the distances between \mathcal{X}_s and $\{\hat{z}\}_{k=1}^K$ as

$$d_k^i(x_s^i, k) = \|f_h(x_s^i; \theta_h) - \hat{z}_k\|_p \quad (1)$$

where p is typically 1 or 2 (L1 or L2 distance). We can score x_s^i by considering an *Aggregation Operator* of either average distance to the cluster centers

$$c_s^i = \frac{1}{K} \sum_{k=1}^K d_k^i \quad (2)$$

or minimum distance

$$c_s^i = \min(\{d_k^i\}_{k=1}^K). \quad (3)$$

To filter, we sort by c_s^i in ascending order and select N' images to create $\mathcal{D}'_s \in \mathcal{D}_s$ and pre-train θ_t on it.

Advantages of our Method Performing unsupervised clustering ensures that our method is not fundamentally limited to target datasets with image classification task and also

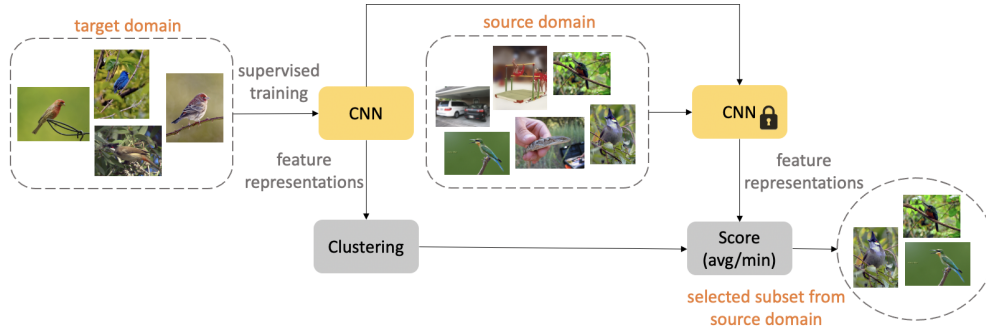


Figure 2: Schematic overview of clustering based filtering. We first train a model on the target domain to extract representations, which we use to cluster the target domain. We score source images with either average or min distance to cluster centers and then filter.

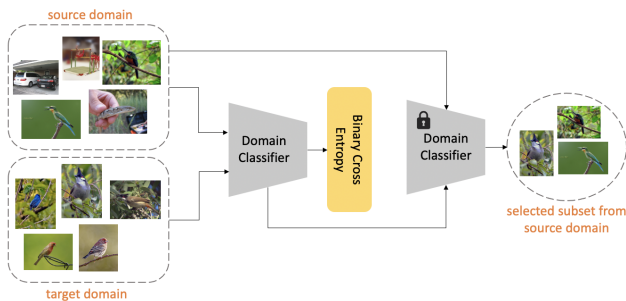


Figure 3: Depiction of the Domain Classifier. We train a simple binary classifier to discriminate between source and target domain and then use the output probabilities on source images to filter.

does not assume that source dataset images in the same class should be grouped together. Furthermore, our method requires only a relatively cheap single forward pass through the pre-training dataset. It attains our goals of efficiency and flexibility, in contrast to prior work such as [11, 7]. We outline the algorithm step-by-step in Algorithm 1 and lay out the method visually in Figure 2.

Algorithm 2 Data Classifier Filtering

- 1: **procedure** DATACLSFILTER($\mathcal{D}_s, \mathcal{D}_t, N'$)
 - 2: SAMPLE $\{x_s^i\}_{i=1}^M \in \mathcal{D}_s$
 - 3: $\mathcal{X}_h \leftarrow \{\{x_s^i\}_{i=1}^M, \{x_t^i\}_{i=1}^M\}$
 - 4: $\mathcal{Y}_h \leftarrow \{\{-1\}_{i=1}^M, \{1\}_{i=1}^M\}$ ▷ Domain Labels
 - 5: $\mathcal{D}_h \leftarrow (\mathcal{X}_h, \mathcal{Y}_h)$ ▷ Training Data
 - 6: $f_h(x; \theta_h) \leftarrow \operatorname{argmin}_{\theta_h} CE_{Loss}(\mathcal{D}_h)$ ▷ Fit Model
 - 7: $c_s \leftarrow \{f_h(x_s^i; \theta_h)\}_{i=1}^M$ ▷ Score
 - 8: $\mathcal{D}'_s \leftarrow TOP(\mathcal{D}_s, N', c_s)$ ▷ Filter Source
 - 9: **return** \mathcal{D}'_s ▷ Return the Filtered Subset
-

4.1.2 Conditional Filtering with Domain Classifier

In this section, we propose a novel domain classifier to filter \mathcal{D}_s with several desirable attributes.

Training. In this method, we propose to learn θ_h to ascertain whether an image belongs to \mathcal{D}_s or \mathcal{D}_t . θ_h is learned on a third dataset $\mathcal{D}_h = (\mathcal{X}_h, \mathcal{Y}_h)$ where $\mathcal{X}_h = \{\{x_s^i\}_{i=1}^M, \{x_t^i\}_{i=1}^M\}$, $M = |\mathcal{D}_t|$, consisting of full set of \mathcal{D}_t and a small random subset of \mathcal{D}_s . Each source image $x_s^i \in \mathcal{X}'_s$ receives a negative label and each target image $x_t^i \in \mathcal{X}_t$ receives a positive label giving us the label set $\mathcal{Y}_h = \{\{0\}_{i=1}^M, \{1\}_{i=1}^M\}$. We then learn θ_h on \mathcal{D}_h using cross entropy loss as

$$\operatorname{argmin}_{\theta_h} - \sum_{i=1}^{2M} y_h^i \log(f_h(x_h^i; \theta_h)) + (1 - y_h^i) \log(1 - f_h(x_h^i; \theta_h)). \quad (4)$$

Scoring and Filtering. Once we learn θ_h we obtain the confidence score $p(y_h = 1|x_s^i; \theta_h)$ for each image $x_s^i \in \mathcal{X}_s$. We then sort the source images \mathcal{X}_s in descending order based on $p(y_h = 1|x_s^i; \theta_h)$ and choose the top N' images to create the subset $\mathcal{D}'_s \in \mathcal{D}_s$.

Interpretation. Our method can be interpreted as selecting images from the pre-training domain with high probability of belonging to the target domain. In a similar direction, [13] shows that the Bayes Optimal binary classifier \hat{f}_h assigns probability

$$p(y_h = 1|x_s^i; \theta_h) = \frac{p_t(x_s^i)}{p_s(x_s^i) + p_t(x_s^i)} \quad (5)$$

for an image $x_s^i \in \mathcal{X}_s$ to belong to the target domain, where p_t and p_s are the true data probability distributions for the target and source domains respectively.

Classifier Calibration. Our domain classifier can be augmented by improving the calibration of f_h with a technique such as temperature scaling [14] or focal loss [25] and using these improved estimates to perform importance

sampling bias correction during pre-training, as explained in [13]. However, we find that the method still works very well on a wide range of tasks and datasets without any further tuning, an attractive factor when considering flexibility and efficiency. We outline the algorithm step-by-step in Algorithm 2 and provide a depiction in Figure 3.

4.2. Adjusting Pre-training Spatial Resolution

To augment our methods, we propose changing spatial resolution of images \mathcal{X}_s in the source dataset \mathcal{D}_s while pre-training. We assume that an image is represented as $x_s^i \in \mathbb{R}^{W_s \times H_s}$ or $x_t^i \in \mathbb{R}^{W_t \times H_t}$ where W_s, W_t , where H_s and H_t represent image width and height. Traditionally, after augmentations, we use $W_s, W_t = 224$ and $H_s, H_t = 224$. Here, we consider decreasing W_s and H_s on the pre-training task while maintaining $W_t, H_t = 224$ on the target task. It is easy to see that reducing image resolution while pre-training can provide significant speedups by decreasing FLOPs required by convolution operations. Indeed, our experiments show that downsizing image resolution by half $W_s, H_s = 112$ almost halves the pre-training time.

Training on downsized images and testing on higher resolution images has previously been explored. In [35], due to geometric camera effects on standard augmentations, the authors report performance gains by training on lower resolution image and testing on normal resolution. Our setting is not as amenable to the same analysis, as we have separate data distributions \mathcal{D}_s and \mathcal{D}_t captured under different settings, and we perform the same training augmentations during both pre-training and finetuning. Nevertheless, we show low resolution training is still an effective method in the transfer learning setting.

5. Experiments

Dataset	#classes	#train	#test
Stanford Cars [43]	196	8143	8041
Caltech Birds [24]	200	6000	2788
Functional Map of the World [6]	62	18180	10609

Table 1: We use three challenging visual categorization datasets to evaluate the proposed pre-training strategies on target classification tasks.

In all experiments, we report finetuning performance for each combination of resolution, pre-training budget, and filtering method. For context, we also report performance with full pre-training and no pre-training.

5.1. Datasets

5.1.1 Source Dataset

We test and validate our methods in a wide range of settings. For our source dataset, we utilize ImageNet-2012 [8], with ~ 1.28 M images over 1000 classes. Downstream tasks include fine grained classification, more general classification, and object detection. We experiment under two data budgets, limiting filtered subsets to 75K ($\sim 6\%$) and 150K ($\sim 12\%$) ImageNet images. This is an appropriate proportion when dealing with pre-training datasets on the scale of tens of millions or more images.

5.1.2 Target Datasets

Classification. As target datasets, we utilize the Stanford Cars [43] dataset, the Caltech Birds [24] dataset, and a subset of the Functional Map of the World [6] (fMoW) dataset. We provide basic details about these datasets in Table 1. These datasets lend important diversity to validate the flexibility of our methods. Cars is a dataset with fairly small distribution shift from ImageNet, and pre-training on ImageNet performs well on it [7]. Birds contains a larger shift and a dataset emphasizing natural settings, such as iNat [7, 41], performs better than ImageNet. Finally, fMoW, consisting of overhead satellite images, contains images very dissimilar to ImageNet. Additionally, Birds and Cars are fine grained, discriminating between different species of birds or models of cars, respectively. In contrast, fMoW is much more general, describing buildings or landmarks [31, 36, 40].

Object Detection. [15, 16] show that unsupervised ImageNet pre-training is most effective when paired with challenging downstream tasks like object detection. Therefore, we also perform experiments in the object detection setting to validate the effectiveness and adaptability of our methods in more challenging tasks than classification. We utilize the Pascal VOC [9] dataset for object detection with unsupervised ImageNet pre-training of the base feature extractor.

5.2. Methods

We experiment with clustering based filtering, using $K = 200$ clusters and both average and min distance to cluster centers, as well as our domain classifier method, using ResNet-18 [18] as our classifier. Furthermore, we combine our filtering methods with downsizing pre-training image resolution from 224×224 to 112×112 using bilinear interpolation. We perform filtering on 224×224 source images, but use it for both 224×224 and 112×112 resolution pre-training to assess flexibility, as we want robust methods that do not need to be specifically adjusted to the pre-training setup.



Figure 4: High scoring ImageNet samples selected by all our conditional filtering methods for target datasets Stanford Cars and Caltech Birds.

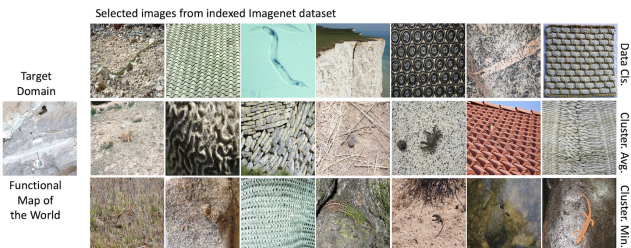


Figure 5: High scoring ImageNet samples selected by all our conditional filtering methods for fMoW.

Efficiency and Adaptability Comparison. For clustering, training a model to extract representations requires training on the target dataset. In comparison, the domain classifier requires training a simpler binary classifier, which we train to achieve 92-95% accuracy in five or fewer epochs. Furthermore, the forward pass for domain classifier based filtering does not require clustering or computing distances and is thus faster than that of clustering based filtering. When the target task is not image level classification, the representation learning step for clustering based filtering must be modified in a non-trivial manner. This can involve a global pool over spatial feature maps while performing object detection or an entirely different setup like unsupervised learning. The domain classifier is more adaptable than clustering as it does not require modification for any type of target task.

Qualitative Analysis. In Figures 4 and 5, we visualize some of the highest scoring filtered images for all our methods on classification tasks and verify that our filtering methods do select images with *relevant features* to the target task. Unsurprisingly, more interpretable images are selected for Birds and Cars, as there are no satellite images in ImageNet. Nevertheless, we see that the selected images for fMoW still contain *relevant features* such as color, texture, and shapes.

5.3. Transfer Learning for Image Recognition

We first apply our methods to the task of image classification with both supervised and unsupervised pre-training. We detail our setup, results, and experiments below.

5.3.1 Experimental Setup

For classification tasks, we train the linear classification layer from scratch and finetune the pre-trained backbone weights.

Supervised Pre-training. For supervised pre-training, in all experiments, we utilize the ResNet-34 model [18] on 1 Nvidia-TITAN X GPU. We perform standard cropping/flipping transforms for ImageNet and the target data. For pre-training, we pretrain on the given subset of ImageNet for 90 epochs, utilizing SGD with momentum .9, weight decay of $1e-4$, and learning rate .01 with a decay of 0.1 every 30 epochs. We finetune for 90 epochs with a learning rate decay of 0.1 every 30 epochs for all datasets. For Cars and Birds, we utilize SGD with momentum .9 [30], learning rate 0.1, and weight decay of $1e-4$. For fMoW, we utilize the Adam optimizer [22] with learning rate $1e-4$.

Unsupervised Pre-training. For unsupervised pre-training, we utilize the state of the art MoCo-v2 [16] technique using a ResNet-50 model [18] in all experiments. We train on 4 Nvidia GPUs. MoCo [15, 16] is a self-supervised learning method that utilizes contrastive learning, where the goal is to maximize agreement between different views of the same image (positive pairs) and to minimize agreement between different images (negative pairs). Our choice to use MoCo is driven by (1) performance, and (2) computational cost. Compared to other self-supervised frameworks, such as SimCLR [3], which require a batch size of 4096, MoCo uses a momentum updated queue of previously seen samples and achieves comparable performance with a batch size of just 256 [15].

We keep the same data augmentations and hyperparameters used in [16]. We finetune the MoCo pre-trained backbone on our target tasks for 100 epochs using a learning

Supervised Pre-train.		Target Dataset			Cost (hrs)
224 x 224		Small Shift	Large Shift		
Pretrain. Sel. Method		Cars	Birds	fMow	
0%	Random Init.	52.89	42.17	43.35	0
100%	Entire Dataset	82.63	74.87	59.05	160-180
6%	Random	72.2	57.87	50.25	30-35
	Data Cls.	74.37	59.73	51.17	35-40
	Clustering (Avg)	73.64	56.33	51.14	40-45
	Clustering (Min)	74.23	57.67	50.27	40-45
12%	Random	76.12	62.73	53.28	45-50
	Data Cls.	76.18	64	53.41	50-55
	Clustering (Avg)	77.12	61.73	53.12	55-60
	Clustering (Min)	75.81	64.07	52.91	55-60

Supervised Pre-train.		Target Dataset			Cost (hrs)
112 x 112		Small Shift	Large Shift		
Pretrain. Sel. Method		Cars	Birds	fMow	
0%	Random Init	52.89	42.17	43.35	0
100%	Entire Dataset	83.78	73.47	57.39	90-110
6%	Random	72.76	57.4	49.73	15-20
	Data Cls.	73.66	58.73	50.66	20-25
	Clustering (Avg)	74.53	56.97	51.32	25-30
	Clustering (Min)	71.72	58.73	49.06	25-30
12%	Random	75.4	62.63	52.59	30-35
	Data Cls.	76.36	63.5	53.37	35-40
	Clustering (Avg)	77.53	61.23	52.67	40-45
	Clustering (Min)	76.36	63.13	51.6	40-45

Table 2: Target task accuracy and approximate filtering and pre-training cost(time in hrs on 1 GPU) on 3 visual categorization datasets obtained by pre-training the ResNet-34 network on different subsets of the source dataset (ImageNet) with different filtering methods at different resolutions.

MoCo-v2 [16]		Target Dataset			Cost (hrs)
224 x 224		Small Shift	Large Shift		
Pretrain. Sel. Method		Cars	Birds	fMow	
0%	Random Init.	52.89	42.17	43.35	0
100%	Entire Dataset	83.52	67.49	56.11	170-180
6%	Random	75.70	56.82	52.53	20-25
	Data Cls.	78.67	61.55	52.96	23-28
	Clustering (Avg)	78.66	60.88	53.19	25-30
	Clustering (Min)	79.45	59.36	53.5	25-30
12%	Random	75.66	61.70	53.56	30-35
	Data Cls.	78.68	63.08	54.01	33-38
	Clustering (Avg)	78.68	62.53	54.4	35-40
	Clustering (Min)	79.55	63.6	54.26	35-40

MoCo-v2 [16]		Target Dataset			Cost (hrs)
112 x 112		Small Shift	Large Shift		
Pretrain. Sel. Method		Cars	Birds	fMow	
0%	Random Init	52.89	42.17	43.35	0
100%	Entire Dataset	84.09	66.57	56.83	100-110
6%	Random	75.38	56.63	52.59	10-15
	Data Cls.	76.84	57.93	53.3	13-18
	Clustering (Avg)	76.86	58.4	53.75	15-20
	Clustering (Min)	77.53	57.1	53.83	15-20
12%	Random	78.35	61.50	54.28	15-20
	Data Cls.	80.38	63.93	54.53	18-23
	Clustering (Avg)	80.21	63.50	55.06	20-25
	Clustering (Min)	79.63	62.77	55.03	20-25

Table 3: Target task accuracy and approximate filtering and pre-training cost(time in hrs on 4 GPUs) on 3 visual categorization datasets obtained by pre-training the ResNet-50 network (using MoCo-v2 [16]) on different subsets of the source dataset (ImageNet) with different filtering methods at different resolutions

rate of 0.001, batch size of 64, SGD optimizer for Cars and Birds, and Adam optimizer for fMoW.

5.3.2 Supervised Pre-training Results

We present target task accuracy for all our methods on Cars, Birds, and fMoW along with approximate pre-training and filtering time in Table 2.

Effect of Image Resolution. We see that downsizing pre-training resolution by a factor of 2 produces gains of up to .5% in classification accuracy on Cars and less than 1% drop in accuracy on Birds and fMoW, while being 30-50% faster than full pre-training. These trends suggest that training on lower resolution images can help the model learn more generalizable features for similar source and target distributions. This effect erodes slightly as we move

out of distribution, however pre-training on lower resolution images offers an attractive trade-off between efficiency and accuracy in all settings.

Impact of Filtering. We find that our filtering techniques consistently provide up to a 2.5% performance increase over random selection, with a relatively small increase in cost w.r.t random selection. Unsurprisingly, filtering provides the most gains on Cars and Birds where the target dataset has a smaller shift. On fMoW, it is very hard to detect *similar* images to ImageNet, as the two distributions have very little overlap. Nevertheless, in this setting, our filtering methods can still select enough relevant features to provide a 1-2% boost in most cases.

Comparison of Filtering Methods. While all our methods perform well, applying a finer lens, we see that the domain classifier is less variable than clustering and always

outperforms random selection. On the other hand, average clustering performs well on Cars or fMoW, but does worse than random on Birds and vice versa for min clustering. These methods rely on computing high dimensional vector distances to assign a measure of similarity and are susceptible to the usual associated pitfalls of outliers and the curse of dimensionality, which may explain their volatility when such high dimensional distances are not considered while pre-training.

5.3.3 Unsupervised Pre-training Results

We observe promising results in the supervised setting, but as explained, a more realistic and useful setting is the unsupervised setting due to the difficulties inherent in collecting labels on large-scale data. Thus, we use MoCo-v2, one of the state-of-the-art unsupervised learning methods, to pre-train on ImageNet and present results for Cars, Birds, and fMoW in Table 3.

Effect of Image Resolution. We find that in the unsupervised setting, with 150K pre-training images, lower resolution pre-training can maintain or even improve performance as the target distribution shifts. Unsupervised pre-training relies more on high level features than intricate label distributions and thus may be better suited than supervised methods for lower resolution pre-training.

Furthermore, we see that filtering is somewhat more effective when pre-training on 224x224 images when compared to 112x112 pre-training, but performance in the latter scenario is still strong. This affirms the robustness of our filtering methods as we filter on 224x224 images but use this filtered set when performing 112x112 pre-training as well.

Increased Consistency of Clustering. Relative to the supervised setting, clustering based filtering provides more consistent performance boosts across the different settings and datasets. It is possible that clustering based filtering may be well suited for unsupervised contrastive learning techniques, which also rely on high dimensional feature distances.

Impact of Filtering. Our filtering techniques, particularly the domain classifier, primarily aim to separate the image distributions based on the true image distributions $p_s(x)$ and $p_t(x)$ instead of prior work [28] that consider the marginal or conditional source class distributions $p_s(y)$ or $p_s(y|x)$ (which may not even be observable). Due to the emphasis on feature similarity and not label distributions, unsupervised learning takes advantage of our filtering methods more than supervised pre-training. Performance on fMoW, with its large distribution shift, is similar to supervised pre-training, but on Birds and Cars, we see gains of up to 5% over random filtering in the 75K setting and up to 4% in the 150K setting, a larger boost than during supervised pre-training.

On the back of the aforementioned gains, we can achieve performance that is within 1-4% of full unsupervised pre-training but close to 10 times faster, due to filtering and downsizing, a strong performance to cost tradeoff. These results are notable, because, as mentioned, we anticipate that unsupervised learning will be the default method for large-scale pre-training and our methods yield minimal performance loss while saving significant pre-training cost.

5.4. Transfer Learning for Object Detection

Previously we explored image level classification target tasks for conditional pre-training. In this section, we perform experiments on transfer learning for object detection target task. In this direction, we use the Pascal VOC dataset as our target dataset. Object detection requires localization and classification of objects and is usually more challenging than image level classification. This serves as a good test to validate the adaptability and flexibility of our methods.

5.4.1 Experimental Setup

We use a standard setup for object detection with a Faster R-CNN detector with a R50-C4 backbone as in [15, 17, 44]. We pre-train the backbone with MoCo-v2 on the full or filtered subset of ImageNet. We finetune for 24k iterations (~23 epochs) on trainval2007 (~5k images). We evaluate on the VOC test2007 set with the default metric AP50 and the more stringent metrics of COCO-style [26] AP and AP75. For filtering, we use the domain classifier with no modifications and for clustering we use MoCo-v2 on Pascal VOC to learn representations.

5.4.2 Results

We present results in Table 4 using no pretraining and full pretraining, for context, as well as with random filtering and domain classifier based filtering combined with image resolution downsizing from 224x224 to 112x112 in the pre-training dataset.

Effect of Image Resolution. For all three metrics, pre-training on low resolution images produces a marginal decrease in performance, with the usual corresponding 40-50% reduction in training time, confirming the adaptability of pre-training on lower resolution images for a challenging task like object detection. As before, the filtering methods are robust since we see high gains with 112x112 pre-training despite performing the filtering on 224x224 images.

Adaptability Comparison Relative to prior work [7, 46], our clustering method is more adaptable and can be used for object detection as well as image classification. However, it is not as adaptable as the domain classifier since the representation learning step for clustering must be changed for an object detection target task. This

		224x224			112x112		
Pretrain. Sel. Method		AP	AP50	AP75	AP	AP50	AP75
0%	Random Init.	14.51	31.00	11.62	14.51	31.00	11.62
100%	Entire Dataset	43.94	73.05	45.96	43.62	72.56	45.52
6%	Random	29.01	54.02	27.26	28.10	52.82	26.39
	Data Cls.	30.47	56.58	29.04	31.19	56.90	30.43
	Clustering (Avg)	30.61	55.65	28.75	30.13	55.01	29.47
	Clustering (Min)	30.44	56.11	29.46	30.39	55.89	28.18
12%	Random	30.84	52.07	29.15	30.56	56.1	29.04
	Data Cls.	34.41	61.85	33.36	34.98	61.83	35.02
	Clustering (Avg)	32.34	56.24	31.28	32.01	57.16	33.48
	Clustering (Min)	32.58	57.77	31.16	32.96	58.25	33.64

Table 4: Comparison of different filtering methods on transfer learning on Pascal-VOC object detection dataset. The R50-C4 backbone is pretrained on the full set or filtered subset of ImageNet with MoCo-v2 in all cases.

can lead to additional complications for clustering when using unsupervised learning techniques, i.e. MoCo-v2, on very small size target task datasets to learn robust representations.

Performance Comparison We observe that our proposed filtering techniques yield consistent gains of 2-6% (almost 10% in one case) over random filtering. We see that the domain classifier outperforms clustering in almost every scenario, with the effects being especially pronounced when using more pre-training samples. We believe that this can be justified because using MoCo-v2 to learn representations for clustering can be less effective on a small size dataset like Pascal VOC. On the other hand, we do not have to modify the domain classifier and can directly learn representations to predict the domain of the samples.

6. Conclusion

In this study, we presented novel methods to filter pre-training datasets for transfer learning, conditioned on a target dataset. Our methods find samples relevant to a target task to perform pre-training on a filtered source dataset. While previous methods focus solely on transfer learning performance, we consider both efficiency and transfer learning performance. Our methods can be applied to source datasets with and without labels as well as target tasks including image classification and object detection. Our experiments show that, given a pre-training data budget, our filtering methods achieve superior performance over random filtering on both classification and object detection, with minimal extra cost. Additionally, we discover that decreasing pre-training image resolution by a factor of four shortens pre-training cost by 30-50% with no drop in target task performance. Finally, relative to supervised pre-training, our filtering methods benefit more from unsuper-

vised pre-training, due to our focus on identifying relevant features, not classes. This positions our methods to be effective on extremely large-scale datasets with no annotations.

References

- [1] William H Beluch, Tim Genewein, Andreas Nürnberger, and Jan M Köhler. The power of ensembles for active learning in image classification. In *Proceedings of the IEEE Conference on Computer Vision and Pattern Recognition*, pages 9368–9377, 2018. 2
- [2] Mathilde Caron, Ishan Misra, Julien Mairal, Priya Goyal, Piotr Bojanowski, and Armand Joulin. Unsupervised learning of visual features by contrasting cluster assignments. *Advances in Neural Information Processing Systems*, 33, 2020. 1
- [3] Ting Chen, Simon Kornblith, Mohammad Norouzi, and Geoffrey Hinton. A simple framework for contrastive learning of visual representations. *arXiv preprint arXiv:2002.05709*, 2020. 1, 2, 6
- [4] Xinlei Chen, Haoqi Fan, Ross Girshick, and Kaiming He. Improved baselines with momentum contrastive learning. *arXiv preprint arXiv:2003.04297*, 2020. 1, 2
- [5] Xinlei Chen, Haoqi Fan, Ross Girshick, and Kaiming He. Improved baselines with momentum contrastive learning. *arXiv preprint arXiv:2003.04297*, 2020. 2
- [6] Gordon Christie, Neil Fendley, James Wilson, and Ryan Mukherjee. Functional map of the world. In *Proceedings of the IEEE Conference on Computer Vision and Pattern Recognition*, pages 6172–6180, 2018. 5
- [7] Yin Cui, Yang Song, Chen Sun, Andrew Howard, and Serge Belongie. Large scale fine-grained categorization and domain-specific transfer learning. In *Proceedings of the IEEE conference on computer vision and pattern recognition*, pages 4109–4118, 2018. 1, 2, 3, 4, 5, 8
- [8] Jia Deng, Wei Dong, Richard Socher, Li-Jia Li, Kai Li, and Li Fei-Fei. Imagenet: A large-scale hierarchical image

- database. In *2009 IEEE conference on computer vision and pattern recognition*, pages 248–255. Ieee, 2009. 1, 2, 5
- [9] Mark Everingham, Luc Van Gool, Christopher KI Williams, John Winn, and Andrew Zisserman. The pascal visual object classes (voc) challenge. *International journal of computer vision*, 88(2):303–338, 2010. 5
- [10] Yarin Gal, Riashat Islam, and Zoubin Ghahramani. Deep bayesian active learning with image data. *arXiv preprint arXiv:1703.02910*, 2017. 2
- [11] Weifeng Ge and Yizhou Yu. Borrowing treasures from the wealthy: Deep transfer learning through selective joint fine-tuning. In *Proceedings of the IEEE conference on computer vision and pattern recognition*, pages 1086–1095, 2017. 1, 2, 3, 4
- [12] Jean-Bastien Grill, Florian Strub, Florent Altché, Corentin Tallec, Pierre Richemond, Elena Buchatskaya, Carl Doersch, Bernardo Avila Pires, Zhaohan Guo, Mohammad Gheshlaghi Azar, et al. Bootstrap your own latent-a new approach to self-supervised learning. *Advances in Neural Information Processing Systems*, 33, 2020. 1
- [13] Aditya Grover, Jiaming Song, Ashish Kapoor, Kenneth Tran, Alekh Agarwal, Eric J Horvitz, and Stefano Ermon. Bias correction of learned generative models using likelihood-free importance weighting. In *Advances in Neural Information Processing Systems*, pages 11058–11070, 2019. 4, 5
- [14] Chuan Guo, Geoff Pleiss, Yu Sun, and Kilian Q Weinberger. On calibration of modern neural networks. *arXiv preprint arXiv:1706.04599*, 2017. 4
- [15] Kaiming He, Haoqi Fan, Yuxin Wu, Saining Xie, and Ross Girshick. Momentum contrast for unsupervised visual representation learning. *arXiv preprint arXiv:1911.05722*, 2019. 1, 2, 5, 6, 8
- [16] Kaiming He, Haoqi Fan, Yuxin Wu, Saining Xie, and Ross Girshick. Momentum contrast for unsupervised visual representation learning. In *Proceedings of the IEEE/CVF Conference on Computer Vision and Pattern Recognition*, pages 9729–9738, 2020. 1, 2, 5, 6, 7
- [17] Kaiming He, Georgia Gkioxari, Piotr Dollár, and Ross Girshick. Mask r-cnn. In *Proceedings of the IEEE international conference on computer vision*, pages 2961–2969, 2017. 8
- [18] Kaiming He, Xiangyu Zhang, Shaoqing Ren, and Jian Sun. Deep residual learning for image recognition. In *Proceedings of the IEEE conference on computer vision and pattern recognition*, pages 770–778, 2016. 5, 6
- [19] Dan Hendrycks, Kimin Lee, and Mantas Mazeika. Using pre-training can improve model robustness and uncertainty. *arXiv preprint arXiv:1901.09960*, 2019. 1, 2
- [20] Geoffrey Hinton, Oriol Vinyals, and Jeff Dean. Distilling the knowledge in a neural network. *arXiv preprint arXiv:1503.02531*, 2015. 2
- [21] Minyoung Huh, Pulkit Agrawal, and Alexei A Efros. What makes imagenet good for transfer learning? *arXiv preprint arXiv:1608.08614*, 2016. 1, 2
- [22] Diederik P Kingma and Jimmy Ba. Adam: A method for stochastic optimization. *arXiv preprint arXiv:1412.6980*, 2014. 6
- [23] Simon Kornblith, Jonathon Shlens, and Quoc V Le. Do better imagenet models transfer better? In *Proceedings of the IEEE conference on computer vision and pattern recognition*, pages 2661–2671, 2019. 1, 2
- [24] Jonathan Krause, Michael Stark, Jia Deng, and Li Fei-Fei. 3d object representations for fine-grained categorization. In *Proceedings of the IEEE international conference on computer vision workshops*, pages 554–561, 2013. 5
- [25] Tsung-Yi Lin, Priya Goyal, Ross Girshick, Kaiming He, and Piotr Dollár. Focal loss for dense object detection. In *Proceedings of the IEEE international conference on computer vision*, pages 2980–2988, 2017. 4
- [26] Tsung-Yi Lin, Michael Maire, Serge Belongie, James Hays, Pietro Perona, Deva Ramanan, Piotr Dollár, and C Lawrence Zitnick. Microsoft coco: Common objects in context. In *European conference on computer vision*, pages 740–755. Springer, 2014. 8
- [27] Dhruv Mahajan, Ross Girshick, Vignesh Ramanathan, Kaiming He, Manohar Paluri, Yixuan Li, Ashwin Bharambe, and Laurens van der Maaten. Exploring the limits of weakly supervised pretraining. In *Proceedings of the European Conference on Computer Vision (ECCV)*, pages 181–196, 2018. 1, 2
- [28] Jiquan Ngiam, Daiyi Peng, Vijay Vasudevan, Simon Kornblith, Quoc V Le, and Ruoming Pang. Domain adaptive transfer learning with specialist models. *arXiv preprint arXiv:1811.07056*, 2018. 1, 2, 3, 8
- [29] Mijung Park and Jonathan Pillow. Bayesian active learning with localized priors for fast receptive field characterization. *Advances in neural information processing systems*, 25:2348–2356, 2012. 2
- [30] Ning Qian. On the momentum term in gradient descent learning algorithms. *Neural networks*, 12(1):145–151, 1999. 6
- [31] Vishnu Sarukkai, Anirudh Jain, Burak Uzkent, and Stefano Ermon. Cloud removal from satellite images using spatiotemporal generator networks. In *The IEEE Winter Conference on Applications of Computer Vision*, pages 1796–1805, 2020. 5
- [32] Ozan Sener and Silvio Savarese. Active learning for convolutional neural networks: A core-set approach. *arXiv preprint arXiv:1708.00489*, 2017. 2
- [33] Evan Sheehan, Burak Uzkent, Chenlin Meng, Zhongyi Tang, Marshall Burke, David Lobell, and Stefano Ermon. Learning to interpret satellite images using wikipedia. *arXiv preprint arXiv:1809.10236*, 2018. 1
- [34] Hoo-Chang Shin, Holger R Roth, Mingchen Gao, Le Lu, Ziyue Xu, Isabella Nogues, Jianhua Yao, Daniel Mollura, and Ronald M Summers. Deep convolutional neural networks for computer-aided detection: Cnn architectures, dataset characteristics and transfer learning. *IEEE transactions on medical imaging*, 35(5):1285–1298, 2016. 1, 2
- [35] Hugo Touvron, Andrea Vedaldi, Matthijs Douze, and Hervé Jégou. Fixing the train-test resolution discrepancy. In *Advances in Neural Information Processing Systems*, pages 8252–8262, 2019. 5
- [36] Burak Uzkent and Stefano Ermon. Learning when and where to zoom with deep reinforcement learning. In *Proceedings of*

- the IEEE/CVF Conference on Computer Vision and Pattern Recognition*, pages 12345–12354, 2020. 5
- [37] Burak Uzkent, Aneesh Rangnekar, and Matthew J Hoffman. Tracking in aerial hyperspectral videos using deep kernelized correlation filters. *IEEE Transactions on Geoscience and Remote Sensing*, 57(1):449–461, 2018. 2
- [38] Burak Uzkent, Evan Sheehan, Chenlin Meng, Zhongyi Tang, Marshall Burke, David Lobell, and Stefano Ermon. Learning to interpret satellite images in global scale using wikipedia. *arXiv preprint arXiv:1905.02506*, 2019. 1, 2
- [39] Burak Uzkent, Evan Sheehan, Chenlin Meng, Zhongyi Tang, Marshall Burke, David B Lobell, and Stefano Ermon. Learning to interpret satellite images using wikipedia. In *IJCAI*, pages 3620–3626, 2019. 2
- [40] Burak Uzkent, Christopher Yeh, and Stefano Ermon. Efficient object detection in large images using deep reinforcement learning. In *The IEEE Winter Conference on Applications of Computer Vision*, pages 1824–1833, 2020. 5
- [41] Grant Van Horn, Oisin Mac Aodha, Yang Song, Yin Cui, Chen Sun, Alex Shepard, Hartwig Adam, Pietro Perona, and Serge Belongie. The inaturalist species classification and detection dataset. In *Proceedings of the IEEE conference on computer vision and pattern recognition*, pages 8769–8778, 2018. 5
- [42] Keze Wang, Dongyu Zhang, Ya Li, Ruimao Zhang, and Liang Lin. Cost-effective active learning for deep image classification. *IEEE Transactions on Circuits and Systems for Video Technology*, 27(12):2591–2600, 2016. 2
- [43] P. Welinder, S. Branson, T. Mita, C. Wah, F. Schroff, S. Belongie, and P. Perona. Caltech-UCSD Birds 200. Technical Report CNS-TR-2010-001, California Institute of Technology, 2010. 5
- [44] Yuxin Wu, Alexander Kirillov, Francisco Massa, Wan-Yen Lo, and Ross Girshick. Detectron2. <https://github.com/facebookresearch/detectron2>, 2019. 8
- [45] Michael Xie, Neal Jean, Marshall Burke, David Lobell, and Stefano Ermon. Transfer learning from deep features for remote sensing and poverty mapping. *arXiv preprint arXiv:1510.00098*, 2015. 1, 2
- [46] Xi Yan, David Acuna, and Sanja Fidler. Neural data server: A large-scale search engine for transfer learning data. In *Proceedings of the IEEE/CVF Conference on Computer Vision and Pattern Recognition (CVPR)*, June 2020. 1, 2, 8